Half-metallic semiDirac point generated by quantum confinement in TiO_2/VO_2 nanostructures

Victor Pardo[1, 2] and Warren E. Pickett[1]

[1]*Department of Physics, University of California, Davis, CA 95616*
[2]*Departamento de Física Aplicada, Universidade de Santiago de Compostela, E-15782 Santiago de Compostela, Spain*

Multilayer VO_2/TiO_2 nanostructures (d^1 - d^0 interfaces with no polar discontinuity) are studied with first principles density functional methods including structural relaxation. Quantum confinement of the *half metallic* VO_2 slab within insulating TiO_2 produces an unexpected and unprecedented two-dimensional new state, with a *semiDirac* point Fermi surface: spinless charge carriers are effective-mass like along one principal axis, but are massless along the other. Effects of interface imperfection are addressed.

VO_2 is a magnetic oxide that undergoes a metal-insulator transition[1] upon lowering the temperature through 340 K, accompanied of a symmetry-breaking structural transition from the high temperature metallic rutile phase[2]. The insulating state takes place via a dimerization of the V-V chains[3]. The origin of this metal-insulator transition is the focus of much recent theoretical activity and remains uncertain. It could be due to the formation of a Peierls state[4, 5], or it could be driven by correlations[6, 7], or more likely may have some mixed origin [8, 9]. TiO_2 is isostructural (in one of its phases) and is a d^0 non-magnetic insulator that is very important industrially and is well understood.

The interface (IF) between a correlated insulator and a band insulator has been recognized as fertile ground for new behavior,[10, 11] and the $LaTiO_3$/$SrTiO_3$ (LTO/STO) IF involving the Mott insulator LTO has attracted much of the theoretical study to date.[12–14] For IFs between band insulators, $LaAlO_3$/$SrTiO_3$ (LAO/STO) has received a great deal of attention.[15–19] In both cases there is a polar discontinuity across the IF, and this aspect has been expected to dominate the resulting behavior, and lead to unexpected phenomena.

The (001) VO_2/TiO_2 IF has been studied by photoemission spectroscopy (PES),[20] which found the IF is insulating when the VO_2 substrate is insulating. PES also has uncovered[21] spectral weight transfer in VO_2/TiO_2 thin films indicating strong correlation effects even for conducting VO_2. Much of the focus on this nanostructure has been on tuning the VO_2 metal-insulator transition temperature[22], because of its potential technological applications. It has been found that a minimum thickness of 5 nm of VO_2 is needed to sustain a metal-insulator transition, for thinner VO_2 layers the transition no longer occurs[23] (the VO_2 layer remains conducting). The explanation is that the insulating state requires a collective structural dimerization along the rutile c-axis that is inhibited by confinement for thinner layers. Since the IF is not polar and the lattice mismatch is small (1 %), structural relaxation is not expected to be severe. Any unusual behavior of this multilayer (ML) will require different microscopic mechanisms than have been uncovered before.

In this paper we present a theoretical study of the electronic behavior of the multilayer (ML) nanostructures $(TiO_2)_n$/$(VO_2)_m$, denoted (n/m), looking in particular at the evolution of the conduction and magnetic properties with VO_2 layer thickness. Since VO_2 is the component that is potentially conducting, we focus on thin VO_2 layers which will incorporate any consequences of quantum confinement. The properties are found to depend strongly on layer thickness and the effects of quantum confinement at small thicknesses give rise to a new electronic state for certain MLs.
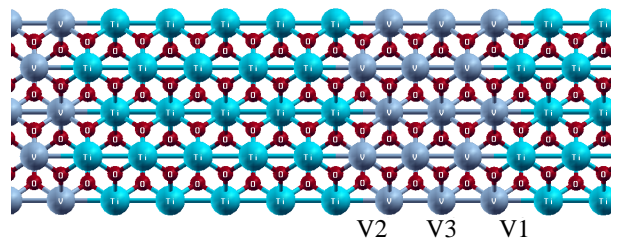

FIG. 1: (Color online) Structure of the 5/3 TiO_2/VO_2 supercell corresponding to growth along the (001) axis, which is the metal chain direction of the rutile structure. V1, V2, V3 label the V ion sites beginning from the one nearest to TiO_2. (Due to a symmetry with respect to the center of the VO_2 slab, the V layers are V1-V2-V3-V3-V2-V1.)

Starting from an average rutile structure of (n/m) MLs, we performed volume and c/a optimization and an internal relaxation of the atomic positions of all the atoms. The main modification is lattice strain along the c axis, interpolating between the slightly
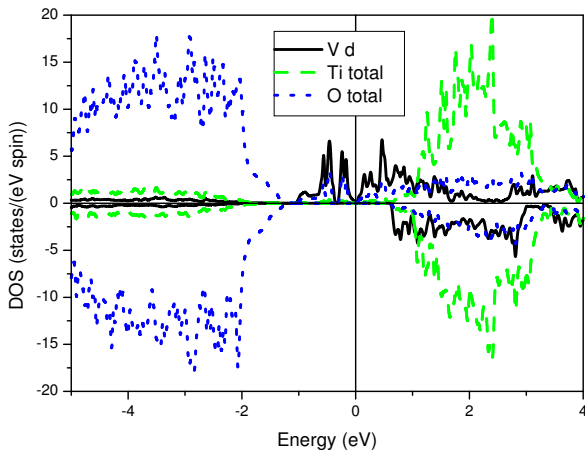
FIG. 2: (Color online) Total density of states in the 5/3 multilayer, showing the location of the V and Ti bands relative to those of O (which are unpolarized). The occupied majority spin bands (plotted upward) lie within a 2 eV gap in the minority spin.

different c lattice constants. We have studied several MLs, varying both TiO_2 and VO_2 layer thicknesses, following identical procedures. Our electronic structure calculations were performed within density functional theory[24] using the all-electron, full potential code WIEN2K[25] based on the augmented plane wave plus local orbital (APW+lo) basis set.[26] The exchange-correlation potential utilized to deal with possible strong correlation effects was the LSDA+U scheme[27, 28] including an on-site U and J (on-site Coulomb repulsion and exchange strengths) for the Ti and V $3d$ states. The values U=3.4 eV, J= 0.7 eV have been used to deal properly with correlations in this multilayered structure; these values are comparable (slightly smaller) than what have been used for bulk VO_2.[9, 29, 30]

While we have studied a variety of n/m (001) MLs, we focus primarily on the (5/3) ML (1.5 nm TiO_2, 0.9 nm of VO_2). The structure, and the identification of the three distinct V sites, is shown in Fig. 1. In terms of distance from the TiO_2 layer, the V ions are labeled V1, V2, V3. The tetragonal symmetry of the rutile structure has been retained in the $x - y$ plane.

V $3d$ bands (Fig. 2) dominate the spectrum close to the Fermi level (E_F), and only three TiO_2 cells are required to give negligible k_z dispersion and thus confine the $3d$ states to a two dimensional (2D) system. FM alignment of the spins is preferred, and half metallicity results. Enlargement of the density of states (DOS) (not shown) reveals vanishing of the DOS precisely at E_F, with no V1 participation just below E_F. This curious vanishing of the DOS reflects a zero gap semiconductor involving V2 and V3 ion states.

The majority spin band structure along high symmetry directions shown in Fig. 3 clarifies an unexpected and unprecendented electronic state. Two bands cross the Fermi level at a single point along the zone diagonal at the point $k_{sD}=(\pm0.37, \pm0.37)\pi/a$ (the precise position of k_{sD} along the (1,1) direction depends on the value of U). Inspection throughout the zone confirms that this Fermi surface crossing is a single point (rather, four symmetry related points), as is the Dirac point in graphene.[31] This single point determines the Fermi energy, again as in graphene.[32] The crossing of the bands precisely at E_F is therefore not accidental, rather it is topologically determined: there are exactly six filled bands below this point, containing the majority spin electrons of each of the six V ions in the cell.

These two bands crossing E_F involve separately V2 and V3 ion $3d$ states, as is illustrated with the color coded fatbands in Fig. 3. With no contribution from the IF ion V1, the dominance of the interior ions V2 and V3 identifies this as a *quantum confinement effect* rather than an IF phenomenon. In Fig. 3 we provide a surface plot of these two band energies in a small region in k-space centered on the band crossing point k_{sD}. This state results only after the ion positions are relaxed, and arises due to band reordering at $k=0$ that occurs during the relaxation. The surface plot reveals yet another peculiarity: while the dispersion is linear along the (1,1) direction as is clear from the band plot, the dispersion is *quadratic* perpendicular to the diagonal; the gap opens due to the loss of symmetry of the two bands off the diagonal $k_x = k_y$, and does so quadratically. To differentiate this point from the graphene Dirac point, we refer to it as the (half metallic) semiDirac (sD) point. The corresponding mass tensor shows extreme anisotropy (zero to normal values), as does the velocity (1.5×10^7 cm/s to zero).[31] This very strongly anisotropic dispersion, between extremes (normal values, to zero) will give rise to peculiar transport and thermodynamic properties, which will be reported separately.

The constant energy surfaces for both electrons and holes are plotted in the right panel of Fig. 3 for low energies in a small region around k_{sD}. The conduction band has a flatness that opens a path for a Fermi surface to develop as a ring around the M=(π, π) point at very low electron doping. The valence band shows iso-energetic contours with an elliptical shape, with the longer axis perpendicular
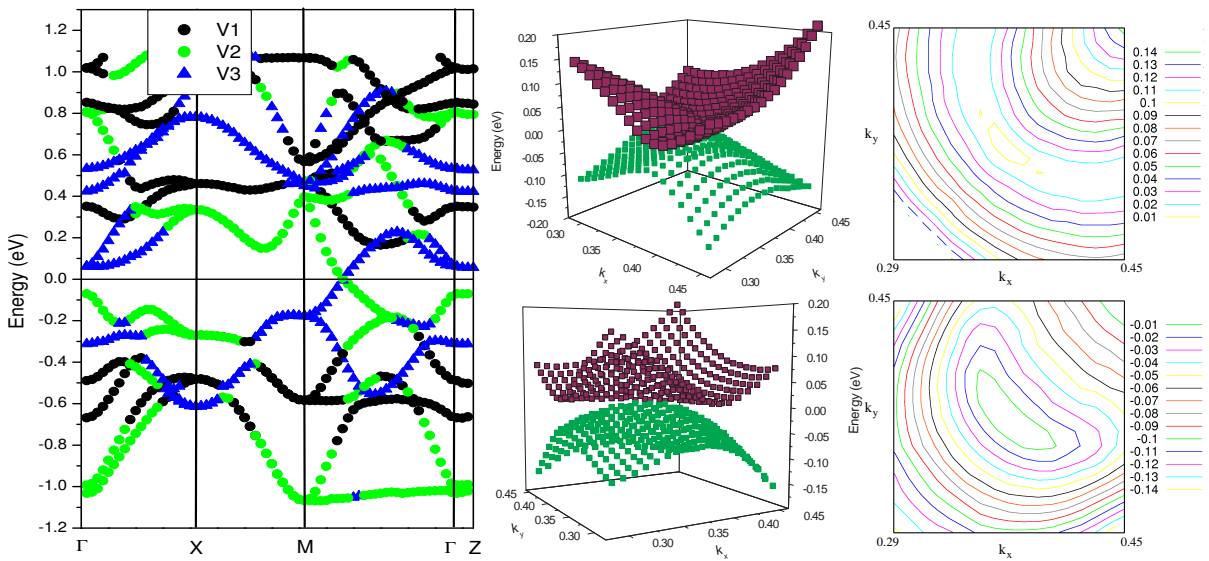
2

FIG. 3: (Color online) Left panel: Blow-up of the band structure around the Fermi level showing in different colors the biggest character of each band. Notice that the two bands crossing at the Fermi level have character from the two most inner V atoms. Note the semiDirac point along the (110) direction where bands cross precisely at the Fermi level. Middle panel: Two different views of the same 'surface' plot of the two bands that cross the Fermi level, centered around the semiDirac point. The valence and conduction bands cross at a single point. The linear dispersion can be seen in the upper plot (upper left and lower right); the quadratic dispersion is clear in the lower panel, where the flatness of the conduction band is also clear. Right panel: contour plots at constant energy (in eV, relative to the Fermi level) of the valence band (below), and the flat conduction band (above) that leads to large M-centered Fermi surfaces.
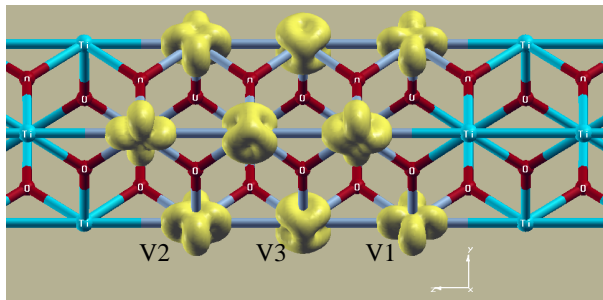
to the zone diagonal.

FIG. 4: (Color online) Spin density plot, isosurface at 0.15 e/Å^3. The particular orbital ordering in a spin-aligned configuration is shown. V1 and V2 have one electron in a $d_\parallel$ and V3 is in a $d_\perp$ orbital.

In bulk VO_2 (V^{4+}: d^1 cations) the distortion from cubic symmetry of the VO_6 octahedron introduces a crystal field (actually, ligand field) that lifts the degeneracy of the t_{2g} orbitals, splitting them into a $d_\parallel$ singlet and two $d_\perp$ orbitals (using Goodenough's notation[4]). The orbital ordering that arises in this 5/3 ML is illustrated by the spin density isosurfaces

in Fig. 4. The V ions (V1 and V2) that terminate a V-V-V chain have an occupied $d_\parallel$ orbital, whereas the chain-center V3 ion has an occupied orbital of $d_\perp \propto d_{xz}+id_{yz}$ character. This orbital ordering is dependent on the magnetic ordering; when the spins along the c direction are antialigned (↑↓↑) the $d_\parallel$ becomes occupied in all sites.

Influence of VO_2 slab thickness. A metal-insulator transition is observed[23] for VO_2 thicknesses above 5 nm (approximately 15 layers), but experimental information on crystalline samples with smaller thickness is space.[33] Our calculations show that the system has an insulating ground state for two layers of VO_2. However, for thicknesses of approximately one nm (3 layers), the material is in the intermediate zero-gap semiDirac state described above, on the brink of metallicity. Thicker VO_2 layers (four or more) become half metallic, a property that is much sought in oxide nanostructures because of its potentially enormous technological applications in spintronic devices.

Influence of magnetic alignment. We have studied antialignment of the moments (ferrimagnetism) along the (001) V-V chains. Such AF coupling is energetically unfavorable in almost all cases. Inter-

estingly, such antialignment changes the orbital ordering: in the 5/3 multilayer (the semiDirac point system when FM), flipping the spin of the intermediate V ion (V2) results in all V ions having an occupied $d_\parallel$ orbital, because the σ-bond along the z-axis between neighboring $d_\parallel$ orbitals favors AF coupling.

Role of V-Ti exchange disorder. States that are very sensitive to disorder are less likely to have importance in applications, since thin film growth does not result in perfectly ordered materials, so we have begun study of the effect of V/Ti exchange near the IF. We find that the most unexpected feature, *i.e.* the development of a half metallic semiDirac point for three VO_2 layers, is robust with respect to two types of ion exchange that do not change the electron count, *i.e.* no doping. The first type was the interchange of V1 with Ti across the IF, which is a typical defect in growth. If we label the Ti sites across the multilayer as Ti1/Ti2/Ti3/Ti4/Ti5/Ti5/Ti4/Ti3/Ti2/Ti1, this first type of disorder corresponds to the interchange of V1 and Ti1, corresponding to a non-abrupt IF. The second type is to interchange V1 with Ti2, which are neighbors along the cation chain. In both cases a semiDirac point persists in spite of changes of the band structure.

To address the robustness of this unusual property in the band structure for the 3-layer VO_2 system, we have varied the thickness of the confining TiO_2 layer. Reduction of the TiO_2 slab thickness to just three layers changes slightly the position of the crossing point in the Brillouin zone, but still gives negligible dispersion along the z-axis, *i.e.* the behavior is still 2D. The semiDirac point is also robust with respect to the strength of correlation effects: the semiDirac point varies along the diagonal from (0.3,0.3) to (0.4,0.4) depending on both the choice of U (for reasonable values, above 2 eV) and TiO_2 thickness.

The finding that quantum confinement in oxide multilayers can produce a semiDirac point at the crossover between insulating and conducting behavior introduces a novel feature in the physics of oxide heterostructures: a polar discontinuity is not required to produce unexpected and unprecedented electronic states in these systems. The conduction behavior, and the changes with doping, for systems with a semiDirac point will be addressed in following papers. We note that oxide nanostructures are mechanically more robust than graphene, which could make patterning of such multilayers possible.

---

[1] F. J. Morin, Phys. Rev. Lett. **3**, 34 (1959).
[2] D. B. McWhan, M. Marezio, J. P. Remeika, and P. D. Dernier, Phys. Rev. B **10**, 490 (1974).
[3] M. Marezio, D. B. McWhan, J. P. Remeika, and P. D. Dernier, Phys. Rev. B **5**, 2541 (1972).
[4] J. B. Goodenough, J. Solid State Chem. **3**, 490 (1971).
[5] R. M. Wentzcovitch, W. W. Chulz, and P. B. Allen, Phys. Rev. Lett. **72**, 3389 (1994).
[6] A. Zylbersztejn and N. F. Mott, Phys. Rev. B **11**, 4383 (1975).
[7] M. S. Laad, L. Craco, and E. Mueller-Hartmann, Europhys. Lett. **69**, 984 (2005).
[8] D. Paquet and P. Leroux-Hugon, Phys. Rev. B **22**, 5284 (1980).
[9] S. Biermann, A. Poteryaev, A. I. Lichtenstein, and A. Georges, Phys. Rev. Lett. **94**, 026404 (2005).
[10] A. Ohtomo, D. A. Muller, J. L. Grazul, and H. Y. Hwang, Nature **419**, 378 (2002).
[11] A. Ohtomo and H. Y. Hwang, Nature **427**, 423 (2004).
[12] D. R. Hamann, D. A. Muller, and H. Y. Hwang, Phys. Rev. B **73**, 195403 (2006).
[13] S. Okamoto, A. J. Millis, and N. A. Spaldin, Phys. Rev. Lett. **97**, 056802 (2006).
[14] R. Pentcheva and W. E. Pickett, Phys. Rev. Lett. **99**, 016802 (2007).
[15] R. Pentcheva and W. E. Pickett, Phys. Rev. B **74**, 035112 (2006).
[16] W. Siemons, et al., Phys. Rev. Lett. **98**, 196802 (2007).
[17] M. S. Park, S. H. Rhim, and A. J. Freeman, Phys. Rev. B **74**, 205416 (2006).
[18] R. Pentcheva and W. E. Pickett, Phys. Rev. B **78**, 205106 (2007).
[19] P. R. Willmott, et al., Phys. Rev. Lett. **99**, 155502 (2007).
[20] K. Maekawa, et al., Phys. Rev. B **76**, 115121 (2007).
[21] K. Okazaki, S. Sugai, Y. Muraoka, and Z. Hiroi, Phys. Rev. B **73**, 165116 (2006).
[22] Y. Muraoka and Z. Hiroi, Appl. Phys. Lett. **80**, 583 (2002).
[23] K. Nagashima, T. Yanagida, H. Tanaka, and T. Kawai, J. Appl. Phys. **101**, 026103 (2007).
[24] P. Hohenberg and W. Kohn, Phys. Rev. **136**, B864 (1964).
[25] K. Schwarz and P. Blaha, Comp. Mat. Sci. **28**, 259 (2003).
[26] E. Sjöstedt, L. Nördstrom, and D. J. Singh, Solid State Commun. **114**, 15 (2000).
[27] V. I. Anisimov, J. Zaanen, and O. K. Andersen, Phys. Rev. B **44**, 943 (2006).

[28] E. R. Ylvisaker, W. E. Pickett, and K. Koepernik, Phys. Rev. B **79**, 035103 (2009).

[29] J. M. Tomczak and S. Biermann, J. Phys.: Condens. Matter **19**, 365206 (2007).

[30] M. W. Haverkort, et al., Phys. Rev. Lett. **95**, 196404 (2005).

[31] K. S. Novoselov, et al., Nature **438**, 197 (2005).

[32] M. I. Katsnelson, Materials Today **10**, 20 (2007).

[33] H. L. M. Chang, et al., J. Physique IV, Colloq. C2 **1**, 953 (1991).